Modeling cyanobacteria life cycle dynamics and historical nitrogen fixation in the Baltic Sea.

Jenny Hieronymus[1], Kari Eilola[1], Malin Olofsson[2], Inga Hense[3], H. E. Markus Meier[4], Elin Almroth-Rosell[1]

5 [1]Department of research and development, Swedish Meteorological and Hydrological Institute, 60175 Norrköping, Sweden
[2]Department of Aquatic Sciences and Assessment, Swedish University of Agricultural Sciences, 750 07 Uppsala, Sweden
[3]Institute of Marine Ecosystem and Fishery Science, Universität Hamburg, 22767 Hamburg, Germany.
[4]Department of Physical Oceanography and Instrumentation, Leibniz Institute for Baltic Sea Research Warnemünde, 18119 Rostock, Germany

Correspondence to: Jenny Hieronymus (jenny.hieronymus@smhi.se)

Abstract. Dense blooms of filamentous diazotrophic cyanobacteria are formed every summer in the Baltic Sea. These autotrophic organisms may bypass nitrogen limitation by performing nitrogen fixation, which also governs surrounding organisms by releasing bioavailable nitrogen. The magnitude of the nitrogen fixation is important to estimate from a

15 management perspective since this might counteract eutrophication reduction measures. Here, a cyanobacteria life cycle model has been implemented for the first time in a high-resolution 3D coupled physical and biogeochemical model of the Baltic Sea spanning the years 1850-2008. The explicit consideration of life cycle dynamics and transitions significantly improves the representation of the cyanobacterial phenological patterns. Compared to earlier 3D-modelling efforts, the rapid increase and decrease of cyanobacteria in the Baltic Sea is well captured by our developed model and is now in concert with

20 observations. The current improvement in timing of cyanobacteria blooms had a large effect on the estimated nitrogen fixation load and is in agreement with *in situ* measurements. By performing four phosphorus sensitivity runs we demonstrate the importance of both organic and inorganic phosphorus availability for historical cyanobacterial biomass estimates. The used model combination can be used to continuously estimate internal nitrogen loads via nitrogen fixation in Baltic Sea ecosystem management, which is of extra importance in a future ocean with changed conditions for the filamentous

25 cyanobacteria.

1 Introduction

Bioavailable nitrogen is globally limiting primary production in the ocean (Moore et al. 2013). Diazotrophic cyanobacteria can bypass this limitation by performing nitrogen fixation. In addition, they may release up to 50 % of its newly fixed nitrogen, which stimulates surrounding organisms (Wannicke et al. 2009, Ploug et al. 2010, 2011). Anthropogenic pressures

30 and climate change synergistically affect the Earth's ecosystems (Steffen et al. 2015). As nitrogen fixing cyanobacteria are suggested to be enhanced by elevated temperatures (Paerl and Huisman 2008, Wannicke et al. 2018), there is an increasing

need to further understand their bloom dynamics and ecosystem impact. For this purpose, combining biogeochemical models and in situ observations is an optimal tool, capturing both temporal and spatial resolution.

35   The Baltic Sea is a semi-enclosed brackish water body and has an early history of multi-stressors and long-term data series, which provides an opportunity to study consequences and possible mitigation strategies for future management of aquatic systems (Reusch et al. 2018). Here, dense blooms of diazotrophic filamentous cyanobacteria are formed every summer (Klawonn et al. 2016, Kahru et al. 2014, Olofsson et al. 2020, 2021), with bloom observations as early as 1854 (Lindström 1855). The blooms as well as the nitrogen fixation are dominated by the filamentous cyanobacterial species *Nodularia*

40   *spumigena*, *Aphanizomenon* sp., and *Dolichospermum* spp. (Klawonn et al. 2016). Future scenarios predict an earlier initiation of the spring bloom, and thus, a potentially prolonged growth period for cyanobacteria in the Baltic Sea (Sommer et al. 2012, Kahru et al. 2016), with demonstrated growth potential even at 4 °C (Olofsson et al. 2019). In addition, results from four decades of monitoring in the Baltic Sea suggest basin-specific changes of the cyanobacteria species due to decreased salinities and elevated temperatures (Olofsson et al. 2020).

45

The processes involved in bloom formation of filamentous cyanobacteria are not yet fully understood (e.g. Conley 2009, Nausch 2012, Wasmund 2012, Wasmund 2017) but recent model studies (Hense and Beckmann (2010), Hense and Burchard, 2010) and observations (Suikkanen et al. 2010) indicate that the life cycle of cyanobacteria plays an important role in determining the timing, duration, and magnitude of the blooms. Including correct seasonal cycles together with spatial

50   variations of cyanobacteria blooms influenced by the different stages of cyanobacteria life cycles will support an improved description of historical changes in biomass and estimates of nitrogen fixation. Hieronymus et al. (2018) demonstrate a temporal shift in cyanobacterial blooms in the model as compared to observations when life cycles are not taken into account. According to Hense et al. (2010b), the rapid increase (or decrease) of the summer concentrations, when using the cyanobacteria life cycle (CLC) model, is a result of transfer between life cycle stages. In the model growing and resting

55   stages are distinguished explicitly, but phosphorus limitation is not considered to describe the bloom dynamics. This is explained by energy limitation despite high temperatures may lead to the formation of resting stages, which need to be further evaluated. Yet, the characteristics of the CLC model have previously only been studied in one dimensional water column setups applied in for the central parts of the Baltic proper.

60   The Baltic Sea is exposed to significant impacts from eutrophication (HELCOM 2010) because of the combination of large increases of nutrient supplies since World War II (Gustafsson et al. 2012), permanent stratification (e.g. Leppäranta 2009), and long water residence times (Meier 2007) that reduce the deep water ventilation and causes wide spread oxygen deficiency. Several large-scale geoengineering interventions have therefore been proposed as solutions to the eutrophication problems (e.g. Conley 2012). Nations around the Baltic Sea have decided on a Baltic Sea Action Plan to reduce external

65   loads of nutrients to the area (HELCOM 2007). Despite reduced nutrient inputs (Gustafsson et al. 2012), there is still an increase in abundance of filamentous cyanobacteria during recent decades (Finni et al. 2001, Kahru and Elmgren 2014, Reusch et al. 2018). The growth of the filamentous cyanobacteria is sensitive to the availability of phosphate (Moisander et al. 2007, Olofsson et al. 2016), and phosphorus loads are therefore of extra importance to decrease to allowable levels suggested by the Baltic Marine Environment Protection Commission HELCOM (2018). With some cyanobacterial taxa

70   being able to utilize both phosphate and organic phosphorus (Schoffeleen et al. 2018) complicates modeling efforts and knowledge on their relative importance is still limited.

The aims of the current study were to gain understanding in phosphorus dynamics in the Baltic proper as well as demonstrate the workings and boundaries of the CLC model in order to use it for continuous monitoring and estimates of nitrogen

75   fixation for management purposes. This will be done by I), run sensitivity experiments addressing phosphorus limitation to determine the optimum settings for the Baltic proper in relation to cyanobacteria blooms, II) include the CLC model in a high-resolution 3D coupled physical and biogeochemical model of the Baltic Sea, and III), validate it to observations of cyanobacteria carbon biomass and estimated nitrogen fixation measurements based on previous *in situ* measurements.

80   **2 Method**

The Baltic Sea is a semi-enclosed estuary which has limited water exchange with the adjacent North Sea (Fig. 1). In order to study bloom formations of filamentous cyanobacteria, we included a modified version of the cyanobacteria life cycle (CLC) model in a high-resolution three dimensional (3D) coupled physical-biogeochemical model of the Baltic Sea (Meier et al. 2003, Eilola et al. 2009, Almroth-Rosell et al. 2011) spanning 1850-2008. The modified CLC model is described in detail

85   below, together with modifications of the biogeochemical model setup (schematically shown in Fig 2).

2.1 Ocean circulation model

The RCO (Rossby Centre Ocean) model is a Bryan–Cox–Semtner primitive equation circulation model with a free surface (Killworth et al., 1991). Its open boundary conditions are implemented in the northern Kattegat, based on prescribed sea level elevation at the lateral boundary (Stevens, 1990). An Orlanski radiation condition (Orlanski1976) is used to address the
90   case of outflow, and the temperature and salinity variables are nudged toward climatologically annual mean profiles to deal with inflows (Meier, 2003). A Hibler-type dynamic–thermodynamic sea ice model (Hibler, 1979) with elastic–viscous–plastic rheology (Hunke and Dukowicz ,1997) and a two-equation turbulence closure scheme of the k-ε type with flux boundary conditions (Meier et al., 2001) is embedded into RCO. The deep-water mixing is assumed inversely proportional to the Brunt–Väisälä frequency, with the proportionality factor based on dissipation measurements in the Eastern Gotland Basin
95   (Lass et al., 2003). RCO is here used with a horizontal resolution of 2 nautical miles (3.7 km) and 83 vertical levels, with a layer thickness of 3 m. RCO allows direct communication between bottom boxes of the step-like topography (Beckmann and Döscher, 1997). A flux-corrected, monotonicity-preserving transport (FCT) scheme is applied in RCO (Gerdes, 1991). RCO has no explicit horizontal diffusion. For further details of the model setup, the reader is referred to (Meier, 2003) and (Meier, 2007).

100

The model performance of temperature and salinity was evaluated in Meier et al. (2018) and conforms well to observations but shows a higher position of the halocline and slightly lower bottom water salinity. The modelled temperature shows good agreement with the observations but some deviations with higher temperatures are found in the upper part of the halocline.

2.2 Biogeochemical model

105   The biogeochemical model SCOBI (Swedish Coastal and Ocean Biogeochemical model) has been developed to study the nutrient cycling in the Baltic Sea (Marmefelt et al., 1999, Eilola et al., 2009, Almroth-Rosell et al., 2011, Almroth-Rosell et al., 2015. SCOBI handles biological and ecological processes in the sea as well as sediment nutrient dynamics and is in this study coupled to RCO (e.g. Eilola et al., 2012, Eilola et al., 2013, Eilola et al., 2014). Resuspension of organic matter is calculated, with the help of a simplified wave model, from the wave and current-induced shear stresses (Almroth-Rosell et
110   al., 2011). SCOBI has a constant carbon (C) to chlorophyll (Chl) ratio C:Chl = 50 (mg C (mg Chl)-1), and the production of phytoplankton assimilates carbon (C), nitrogen (N) and phosphorus(P) according to the Redfield molar ratio (C:N:P = 106:16:1) (Eilola et al., 2009). The molar ratio of a complete oxidation of the remineralized nutrients is O2:C = 138. Dead

organic material, represented by separate variables for nitrogen and phosphorus accumulates in detritus in the water column

and in the sediments. For further details of the "standard" SCOBI model, the reader is referred to Eilola et al. (2009), Eilola

115   et al. (2011) and Almroth-Rosell et al. (2011).

2.3 Cyanobacteria life cycle model

The CLC model we used is a modified version of the detailed life cycle model developed by Hense and Beckmann (2006)

including internal nutrient quotas, and the simplified version by Hense and Beckmann (2010) where life cycle transitions

only depend on external factors. The CLC model equations as well as variables and parameters can be found in the

120   Supplementary material.

Similar to Hense and Beckmann (2006, 2010), we pooled the three main important nitrogen fixing taxa *N. spumigena*,

Aphanizomenon sp. and *Dolichospermum* spp. into one functional cyanobacteria group. We are well aware that there are

differences among the species (e.g. with respect to salinity or temperature dependence) and thus we may not expect to be

125   able to reproduce specific local patterns. Nevertheless, our model will be able to reproduce the main seasonal and spatial

patterns of biomass and nitrogen fixation.

Growth and life cycle transitions in our CLC model depend on external factors, which is similar to Hense and Beckmann

(2010), but we kept the sinking and rising stage separated. We thus distinguish between three life cycle stages: the growing

130   and nitrogen fixing stage (vegetative cells with heterocysts, called HET), the resting stage (akinetes, called AKI) and a stage

(called REC) where we combine the recruiting (cells with gas vesicles) and the growing, non-nitrogen fixing stage

(vegetative cells without heterocysts). HETs are positively buoyant, AKIs in the water (AKIW) are sinking and may end up

in the sediment (AKIB) and RECs are rising. Dead HETs and RECs end up in the pool of dead organic matter. Occasions

with resuspension may transfer AKIB from the sediment to the water AKIW. Life cycle transitions are treated in a relatively

135   simple way: Following Hense and Beckmann. (2010), we use the *in situ* growth rate for the transition between the life cycle

stages HET and AKI. Once the actual growth rate is below a critical threshold, which indicates unfavorable growth

conditions, a transfer into the AKI compartment takes place.

For the transition between AKI (AKIB and AKIW) and REC we prescribe a fixed germination window - from April 20 to

140   the end of April, instead of using a dynamic germination window as proposed by Hense and Beckmann (2010). This is

because the computational costs in a 3D framework are too high. Shifting the germination window, however, has only a small impact on the timing of maximum cyanobacteria abundance in summer and the magnitude of nitrogen fixation. The decadal mean nitrogen fixation is lower when germination is earlier by about 4-7%, while the maximum annual difference found for the entire period 1850-2008 is lower by 14%.

145

Growth of HET and REC are inhibited under anoxic conditions. For potential growth and transition of AKI to REC we assume a salinity dependent window between 3 and 10 PSU which is in fair agreement with the optimum growth of *N. spumigena* (5-10 PSU), *Aphanizomenon* sp. (0-7 PSU) (Rakko and Seppälä, 2014}, and *Dolichospermum* spp. (0-6 PSU) (Teikari et al. 2018). The AKIB is assumed to be rapidly immobilized in the sediment under salinity outside of the defined

150 range. This effect is simulated by very large burial of AKIB when salinity is lower than 3 PSU or higher than 10 PSU. The temperature limitation for the growth of HET and REC (Supplementary material, Table S.3, Eqs. 8 and 26) reaches 10% of its maximum (where maximum equals 1 and indicates least limited) at a temperature of 11°C. The growth is unlimited by temperature at 28°C after which a temperature increase means a decline in growth.

155 **2.4 Model forcing**

The historical simulation uses reconstructed atmospheric, hydrological and nutrient load forcing and daily sea levels at the lateral boundary for the period 1850-2008 as described in detail in Meier et al. (2018) and Gustafsson et al. (2012) and references therein. The used High Resolution Atmospheric Forcing Fields for the period 1850-2008 were reconstructed using atmospheric model data for 1958–2007 together with historical station data of daily sea-level pressure and monthly air

160 temperature observations. For the calculation of monthly mean river flows five different historical data sets were merged. The basin integrated reconstructed nutrient loads from land and atmosphere to the present model are the same as used and described by Gustafsson et al. 2012. Nutrient loads contain both organic and inorganic phosphorus and nitrogen, respectively. In the present SCOBI version, the nitrogen and phosphorus detritus were separated and thus used both organic phosphorus and nitrogen from the forcing. This is the only difference in forcing from the present SCOBI model compared to

165 the model used by Meier et al. 2018, where detritus consisted of one pool limited by the Redfield ratio. Daily mean sea level elevations at the boundary in the Northern Kattegat were calculated from the reconstructed, meridional sea level pressure gradient across the North Sea. In case of inflow, temperature, salinity, nutrients and detritus values were nudged towards

observed climatological seasonal mean profiles for 1980–2005 at the monitoring station Å17 in the southern Skagerrak. Nutrient concentrations before 1900 were assumed to be only 85% of present-day concentrations. A linear decrease of

170   nutrient concentrations from 1950 and back in time to 1900 was assumed.

2.5 Observations

The Swedish National Marine Monitoring Program includes monthly tube sampling of phytoplankton abundance (including filamentous cyanobacteria) and water collection for chemical and physical parameters (e.g. inorganic nutrients, oxygen, salinity, temperature). This data is hosted by the Swedish National Oceanographic Data Centre at the Swedish Hydrological

175   and Meteorological Institute and is freely accessible at www.smhi.se. For this work we have also used data of oxygen and nutrients from The Baltic Environmental Database (BED) which includes post processed monitoring station data from a number of institutes around the Baltic Sea. The data is freely available at http://nest.su.se/bed. The cyanobacteria biovolume (mm3 l-1) is calculated based on cell numbers and size of filaments (Olenina et al. 2006) and further to carbon concentrations (referred to as cyanobacteria biomass) based on Menden-Deuer and Lessard (2000). Concentrations of

180   inorganic nutrients and oxygen were extracted from the database for station BY15 in the Eastern Gotland Basin, and cyanobacteria biomass for four stations in the Baltic proper for 1999-2008 (Fig. 1). The cyanobacteria biovolume was used to estimate nitrogen fixation rates (mmol N m-2 d-1) based on empirical species-specific measurements (Klawonn et al. 2016) according to Olofsson et al. (2021). The estimated nitrogen fixation rates were also calculated to annual nitrogen loads for the Baltic proper during 1999-2008, assuming a size of 200 000 km2, and provided as kton N yr-1.

185   ## 2.6 Phosphorus dependence

In the original model by Hense and Beckmann (2006) that includes also the internal energy and nitrogen, the seasonal changes in cyanobacteria biomass are adequately modelled without taking phosphate into account. The rapid decrease of HET in autumn is then a result of an internal energy crisis caused by the high energy demand of nitrogen fixation together with decreasing temperatures and light. This is true also for the simplified model of Hense and Beckmann (2010) where the

190   growth rate of HET is strongly limited by temperature. However, in the Baltic Sea, the phosphorus concentrations may limit the cyanobacteria biomass (Degerholm et al., 2006). We have therefore performed a series of sensitivity runs to evaluate the role of phosphorus uptake. In the experimental runs, we distinguish between uptake of inorganic and organic phosphorus, since both types are utilized by cyanobacteria (Schoffelen et al. 2018). A preferential uptake of dissolved inorganic

phosphorus is, however, assumed in the model. REC and HET are assumed to assimilate C, N and P, and produce detritus,

195 according to Redfield molar ratios.

In the first experiment (noP), we excluded phosphorus dependence from cyanobacteria in line with Hense and Beckmann (2010). In this case, the cyanobacteria can grow completely independent of phosphate availability in ambient water. In the next experiment (sPlim), we included strong limitations from both phosphate and organic phosphorus. In this case, the half

200 saturation constants are large and the cyanobacteria growth depends strongly on the availability of phosphate.

In the third experiment, we assigned a very small value (10^{-6}) to the half saturation constants of both the phosphate and the organic phosphorus limitation terms, effectively removing the phosphorus limitation of cyanobacteria (wPlim). As long as phosphate exists in small amounts in ambient water, the growth is maintained independent of the concentration. However, in

205 the absence of phosphate the growth is terminated.

In the fourth and final experiment, we kept the limitation by inorganic phosphate but removed the ability to utilize organic phosphorus in cyanobacteria (noOP). As can be deduced from Eq. 1 in Supplementary material, Table. S.3, the growth, in this case, gets no additional reinforcement from organic phosphorus.

210

The differences in parameter values between the phosphorus sensitivity runs are found in Table S.5 in the Supplementary material.

3 Results and discussion

We have used a novel combination of a 3D-model and a cyanobacteria life cycle model (CLC) for the Baltic Sea. In order to

215 determine the optimum phosphorus settings for estimating cyanobacteria biomass and nitrogen fixation rates we performed four phosphorus limitation experiments where after the optimum were used for the estimates and validated to in situ observations.

3.1 Phosphorus sensitivity of cyanobacteria

The simulated biomass was generally larger than observations in all four phosphorus limitation experiments (Fig. 3). The

220 experiment that generated the largest biomass was by far noP which completely excludes the impact of phosphorus in

ambient water. Since the cyanobacteria were not dependent on phosphate or nitrate, they grew extensively even in the first part of the 20th century (Fig. 4) when observations indicate that cyanobacteria blooms were seldom observed (Finni et al, 2001). Up until about 1980, the noOPlim (no additional contribution from organic phosphorus) generally generated the lowest annual mean. After noP, wPlim generated the highest annual mean. This is to be expected as the growth rate, given

225   the same amount of organic and inorganic phosphate, in this case is largest (see Eq. 1 and Eq. 4 in Table S.3). Fig. 4 further displays a decline in cyanobacteria biomass from the mid 20th century to the 1980s for experiment noP. The reason for this decline is most likely the sharp increase in nutrient loads (Gustafsson et al., 2012) generating a competitive advantage of faster growing diatoms and flagellates leaving less DIN for the non-nitrogen fixing RECs . This is indicated also by the increase in diatoms and other phytoplankton biomass accompanying the cyanobacteria decline (Fig. 4, lower panel).

230

The experiments sPlim, wPlim, and noOP generated results closer to observations as compared to noP (Fig. 3). The lowest biomass was generated through wPlim for all stations except BY31. It is notable that wPlim also generated the best bloom timing as compared to observations. This experiment allows cyanobacteria to grow quickly even at low phosphate concentrations as long as the temperature is above approximately 11 degrees C (see Eq. 8 in Table S.3). Thereby the

235   temperature sets the threshold of when the bloom will be initiated, and the phosphate dependence decides the end of it. The noP run generates a start of bloom that is close to wPlim but a later termination. The best seasonal timing validates our use of wPlim in our nitrogen fixation runs.

3.2 Including the cyanobacteria life cycle model

240   To estimate cyanobacteria biomass and nitrogen fixation rates we used the combined 3D and CLC model for the Baltic proper region using the phosphorus limitation setting wPlim based on the limitation experiments. Both, the model results and observations, captured an increase in filamentous cyanobacteria biomass in May-June and with a maximum abundance in July-August (Fig. 3). This is a typical seasonal cycle of cyanobacteria in the Baltic proper (Olofsson et al. 2020), and is an important improvement attained by using this model combination as compared to previous results (Hieronymus et al. 2018).

245   This improved seasonality is due to the inclusion of the cyanobacteria life cycle model (Hense and Beckmann, 2010). In earlier studies using models, the bloom of filamentous cyanobacteria was initiated too late in the season, resulting in a very low nitrogen fixation due to the temperature dependence in the model and decreasing water temperatures during fall (Hieronymus et al. 2018). By obtaining a bloom more constrained to the summer months, a larger nitrogen fixation due to

higher temperatures was observed in the present study. The updated nitrogen fixation rates were also in the same range as

250 estimates based on measurements for the same stations during the years 1999-2008, both in magnitude and timing (Fig. 5).

For nitrogen fixation, there was a slight difference where the model displayed a prolonged peak period in July - August

while the observations showed a peak more contained to July. The strong coherence between model results and observed

nitrogen fixation is somewhat surprising given the larger cyanobacteria biomass displayed by all model experiments

compared to observations (Fig. 3).

255

We estimated the internal nitrogen load via nitrogen fixation to the Baltic proper based on monitoring and in situ

measurements to a mean of 399 kton per year for 1999-2008, but with a large variation among years (SD ± 104). This is

slightly below the external load from river runoff and atmospheric deposition of 430 kton per year (± 54), provided by

HELCOM (2018). For the model combination we used herein, we got an estimated mean nitrogen load of 362 kton per year

260 for experiment wPlim over the same years for the Baltic proper (calculated over an area of 216,600 km2). The estimated

annual nitrogen load via nitrogen fixation to the Baltic proper has not changed over recent years (2013-2017 in Olofsson et

al. 2021), and is in the range of other studies for the Baltic proper (310 kton in Rolff et al. 2007; 370 kton in Wasmund et al.

2001; 396 kton in Svedén et al. 2016) but below the estimated load of 613 kton in Wasmund et al. (2005), 514 kton in

Gustafsson et al. (2013), and 511 kton in Schneider et al. (2009). For the Bothnian Sea, however, the estimated nitrogen load

265 via nitrogen fixation has more than doubled from 1999-2004 until 2012-2017, with an increase in filamentous cyanobacteria

along with decreased salinities (Olofsson et al. 2020).

3.3 Nutrients and oxygen

Diazotrophic cyanobacteria increase bioavailable nitrogen through release of ammonium from its newly fixed nitrogen

(Ploug 2010; 2011). They also impact surrounding organisms by competing for phosphate. We therefore demonstrate the

270 mean seasonal cycle of phosphate and nitrate mean concentrations provided by the model for the periods 1999-2008 and

1960-1980 (Fig. 6). In the earlier period, wPlim consistently generates the highest biomass and noOP the lowest as expected

from the lower growth rate obtained in this case (cf Eq 1., Table S.3). During the later period, dissolved inorganic nitrogen

(DIN; nitrate and ammonium) is completely depleted after the spring bloom providing little opportunity for other

phytoplankton than cyanobacteria to grow (Fig. 6). However, during the earlier part of the run, DIN is available even during

275 summer allowing for higher biomass of the surrounding diatoms and other phytoplankton (Fig. 4). Furthermore, in the early
period, the phosphate concentrations are higher and DIN concentrations lower in wPlim compared to the sPlim and noOP which generates higher cyanobacteria biomass. In the later period, the phosphate concentrations are lowest in wPlim generating a smaller biomass compared to the sPlim and noOP.

280 Fig. 7 shows the surface winter concentration of phosphate and DIN as well as oxygen at 200m depth at monitoring station BY15 for the different runs together with observations. All experiments, with the notable exception of noP, conform well to observed winter surface phosphate. With no phosphorus in cyanobacteria, the winter phosphate concentration becomes too high reflecting the extensive primary production that consumes the deep water oxygen and generates sedimentary phosphate release in this experiment. The 200m oxygen concentration is well captured in all other experiments.

285

The mean vertical profiles of phosphate, DIN and oxygen at stations BY5 and BY15 for experiment wPlim show an overall good representation by the model (Fig. 8). Below the mixed layer, the DIN concentrations are high compared to observations and the phosphate at BY5, a bit too low. The low surface DIN is a reflection of low nitrate concentrations as compared to observations which is also reported by Meier et al. (2012) and Saraiva et al. (2018). The low surface DIN is also seen in Fig.

290 7 where the noP experiment gives rise to higher DIN concentrations as nitrogen fixation due to strong cyanobacteria blooms in this case adds more DIN to the water column. Despite the shortcomings, the trends for both nutrients and oxygen are well captured by the model.

4 Summary and conclusions

295 Through a series of sensitivity experiments, we have shown that the inclusion of a weak phosphate limitation is essential for the CLC model in the Baltic Sea. Excluding this dependence generates too high concentrations of cyanobacteria, especially in the first part of the 20th century when cyanobacteria blooms were rarely observed. The large primary production in this case was also reflected in too high phosphate concentrations as eutrophication induced anoxia which gave rise to sedimentary phosphate release.

300

By including the CLC model into the 3D model for the Baltic proper we demonstrate a clear improvement in seasonality of blooms as compared to previous studies (Hieronymus et al. 2018). The next step in the development of the CLC model would be to instead of one functional type of cyanobacteria include three individual types, more closely capturing the

differences between the dominating taxa (Klawonn et al. 2016). *Aphanizomenon* sp. for example can perform equally high
305 nitrogen fixation rates in 10º C during spring as during the summer (Svedén et al. 2015), and they are responsible for the
highest total nitrogen fixation in the region due to its long growth season (Klawonn et al. 2016). *Aphanizomenon* sp. may
also use different sources of phosphorus, which may further discriminate the growth niches by the filamentous
cyanobacterial species (Shoffelen et al. 2018). Phosphorus cycling is a complex topic, which also needs further studies in
natural ecosystems, as high turnover rates of phosphorus of only about 2 h are hard to trace (Nausch et al. 2018). To include
310 more species in the model might be of extra importance as climate change scenarios can change the community composition
in the future (Wulff et al. 2018; Olofsson et al. 2020).

In this work, we have used a CLC model that includes benthic and pelagic akinetes from which the summer blooms
originate. Research has shown that the life cycles of the different major bloom forming taxa are complex and there is no
315 single answer on how they start growing after winter (Munkes et al. 2021). Experiments have suggested that all taxa form
akinetes to some extent but the summer bloom of *Nodularia spumigena* and *Aphanizomenon* sp. originates mainly from
small, overwintering water column populations while *Dolichospermum* spp. seems to originate from both akinetes and
pelagic filaments (Wasmund et al. 2017, Suikkanen et al., 2010). The large improvement in seasonality when the lifecycle of
cyanobacteria is modelled, as opposed to earlier modelling attempts that include only small winter populations, does
320 however indicate that the separation into different lifecycle stages is of key importance for capturing the start and end of
bloom.

Capturing the seasonality of cyanobacteria blooms is of great importance due to their impact on water quality as well as for
obtaining better estimates of nitrogen fixation that contributes to eutrophication. This work constitutes a step forward for the
325 modelling of cyanobacteria blooms in the Baltic Sea. The inclusion of CLC can with some further development be used to
merge observations and modeling for obtaining better prognostic estimates of cyanobacteria blooms, which can be used for
management purposes.

Code availability

330 The model code of the ocean model used for the simulations is publicly available from the Swedish Meteorological and
Hydrological Institute, Norrköping, Sweden (https://www.smhi.se, E-mail: smhi@smhi.se).

Data availability

Model data displayed in the figures are publicly available with doi:10.5281/zenodo.4980132

335

Supplement link

Author contribution

KE developed the RCO-SCOBI-CLC code and designed the experiments with the help of IH. KE also performed the model
340 runs. MO provided the observational data on cyanobacterial biomass and calculated the estimates of nitrogen fixation based
on previous in situ measurements. HEMM and EAR contributed to the design of the research. JH made the analysis and
prepared the manuscript with input from all co-authors.

Acknowledgments

The research presented in this study is part of the Baltic Earth program (Earth System Science for the Baltic Sea region, see
345 http://www.baltic.earth) and was funded by the Swedish Research Council for Environment, Agricultural Sciences and
Spatial Planning (FORMAS) within the project "Cyanobacteria life cycles and nitrogen fixation in historical reconstructions
and future climate scenarios (1850-2100) of the Baltic Sea" (grant no. 214-2013-1449). Funding was also provided by the
Swedish Research Council (VR) within the project "Reconstruction and projecting Baltic Sea climate variability 1850–2100"
(Grant No. 2012–2117).

350 **References**

Almroth-Rosell, E., Eilola, K., Hordoir, R., Meier, H. E. M., and Hall, P. O. J. (2011). Transport of fresh and resuspended
particulate organic material in the Baltic Sea - a model study. Journal of Marine Systems doi:10.1016/j.jmarsys.2011.02.005

Almroth-Rosell, E., Eilola, K., Kuznetsov, I., Hall, P. O., and Meier, H. E. M. (2015). A new approach to model oxygen
355 dependent benthic phosphate fluxes in the baltic sea. Journal of Marine Systems. doi:10.1016/j.jmarsys.2014.11.007

Beckmann, A. and Döscher, R. (1997). A Method for Improved Representation of Dense Water Spreading over Topography
in Geopotential-Coordinate Models. Journal of Physical Oceanography doi:10.1175/1520-
0485(1997)027h0581:AMFIROi2.0.CO;2
360

Conley, D.J., et al., 2009. Hypoxia-related processes in the Baltic Sea. Environ. Sci. Technol. 43 (10), 3412–3420.

Degerholm, J., Gundersen, K., Bergman, B., & Söderbäck, E. (2006). Phosphorus-limited growth dynamics in two Baltic Sea cyanobacteria, Nodularia sp. and Aphanizomenon sp. FEMS Microbiology Ecology, 58(3), 323–332.
365 https://doi.org/10.1111/j.1574-6941.2006.00180.x

Eilola, K., Almroth-Rosell, E., and Meier, H. E. M. (2014). Impact of saltwater inflows on phosphorus cycling and eutrophication in the Baltic Sea: a 3D model study. Tellus A doi:10.3402/tellusa.v66.23985

370 Eilola, K., Gustafsson, B., Kuznetsov, I., Meier, H. E. M., Neumann, T., and Savchuk, O. (2011). Evaluation of biogeochemical cycles in an ensemble of three state-of-the-art numerical models of the baltic sea. Journal of Marine Systems 88, 267 – 284. doi:https://doi.org/10.1016/j.jmarsys.2011.05.004

Eilola, K., Mårtensson, S., and Meier, H. E. M. (2013). Modeling the impact of reduced sea ice cover in future climate on the
375 Baltic Sea biogeochemistry. Geophysical Research Letters 40, 149–154. doi:10.1029/2012GL054375

Eilola, K., Meier, H. E. M., and Almroth, E. (2009). On the dynamics of oxygen, phosphorus and cyanobacteria in the baltic sea; a model study. Journal of Marine Systems 75, 163 – 184. doi:https://doi.org/10.1016/j.jmarsys.2008.08.009

380 Eilola, K., Rosell, E. A., Dieterich, C., Fransner, F., Höglund, A., and Meier, H. E. M. (2012). Modeling nutrient transports and exchanges of nutrients between shallow regions and the open baltic sea in present and future climate. Ambio doi:10.1007/s13280-012-0322-1

Finni, T., Kononen, K., Olsonen, R., Wallström, K. (2001). The History of Cyanobacterial Blooms in the Baltic Sea.
385 AMBIO: A Journal of the Human Environment, 30(4), 172-178.

Gerdes, R., Köberle, C., and Willebrand, J. (1991). The influence of numerical advection schemes on the results of ocean general circulation models. Climate Dynamics doi:10.1007/BF00210006

390 Gustafsson, Ö.J., Gekting, P., Andersson, U., Larsson, and Roos. P. (2013). An assessment of upper ocean carbon and nitrogen export flux on the boreal continental shelf: A 3-year study in the open Baltic Sea comparing sediment traps, 234Th proxy, nutrient, and oxygen budgets. Limnology and Oceanography Methods 11: 495–510.

Gustafsson, B. G., Schenk, F., Blenckner, T., Eilola, K., Meier, H. E. M., Müller-Karulis, B., Neumann, T., Ruoho-Airola,
395 T., Savchuk, O. P., and Zorita, E. (2012). Reconstructing the development of baltic sea eutrophication 1850-2006. Ambio. https://doi.org/10.1007/s13280-012-0318-x

HELCOM 2018. Inputs of nutrients to the subbasins. HELCOM core indicator report. http://www.helcom.fi/baltic-sea-action-plan/nutrient-reduction-scheme/progress-towards-maximumallowable-inputs/. Accessed Jan 2018.

400

Hense, I. and Beckmann, A. (2006). Towards a model of cyanobacteria life cycle—effects of growing and resting stages on bloom formation of n2-fixing species. Ecological Modelling 195, 205 – 218. doi:https://doi.org/10.1016/j.ecolmodel.2005.11.018

405 Hense, I. and Beckmann, A. (2010). The representation of cyanobacteria life cycle processes in aquatic ecosystem models. Ecological Modelling 221, 2330 – 2338. doi:https://doi.org/10.1016/j.ecolmodel.

Hense, I., & Burchard, H. (2010). Modelling cyanobacteria in shallow coastal seas. Ecological Modelling, 221(2), 238–244. https://doi.org/10.1016/j.ecolmodel.2009.09.006

410

Hibler, W. D. (1979). A Dynamic Thermodynamic Sea Ice Model. Journal of Physical Oceanography. doi:10.1175/1520-0485(1979)009h0815:ADTSIMi2.0.CO;2

Hieronymus, J., et al. 2018.Causes of simulated long-term changes in phytoplankton biomass in the Baltic proper: a wavelet 415 analysis. Biogeosciences. 15: 5113-5129.

Hunke, E. C. and Dukowicz, J. K. (1997). An Elastic–Viscous–Plastic Model for Sea Ice Dynamics. Journal of Physical Oceanography. doi:10.1175/1520-0485(1997)027h1849:AEVPMFi2.0.CO;2

420 Kahru, M., and Elmgren, R. (2014). Multidecadal time series of satellite-detected accumulations of cyanobacteria in the Baltic Sea. Biogeosciences 11: 3619–3633.

Kahru, M., Horstmann, U., and Rud, O. (1994). Satellite detection of increased cyanobacteria blooms in the Baltic sea: Natural fluctuation or ecosystem change? Ambio 23: 469–472.

425

Killworth, P. D., Webb, D. J., Stainforth, D., and Paterson, S. M. (1991). The Development of a Free-Surface Bryan–Cox–Semtner Ocean Model. Journal of Physical Oceanography doi:10.1175/1520-0485.

Klawonn, I., Nahar, N., Walve, J., Andersson, B., Olofsson M., Svedén, J.B., Littmann, S., Whitehouse, M.J., et al. 2016.
430   Cell-specific nitrogen- and carbon-fixation of cyanobacteria in a temperate marine system (Baltic Sea). Environmental
Microbiology 18: 4596–4609.

Lass, H. U., Prandke, H., and Liljebladh, B. (2003). Dissipation in the baltic proper during winter stratification. Journal of
Geophysical Research: Oceans 108. doi:10.1029/2002JC001401
435

Marmefelt, E., Arheimer, B., and Langner, J. (1999). An integrated biogeochemical model system for the Baltic Sea.
Hydrobiologia doi:10.1023/A:1003541816177

Meier, H. E.M., Andersson, H. C., Arheimer, B., Blenckner, T., Chubarenko, B., Donnelly, C., et al. (2012). Comparing
440   reconstructed past variations and future projections of the Baltic Sea ecosystem - First results from multi-model ensemble
simulations. Environmental Research Letters doi:10.1088/1748-9326/7/3/

Meier, H. E. M. (2001). On the parameterization of mixing in three-dimensional Baltic Sea models. Journal of Geophysical
Research: Oceans doi:10.1029/2000JC000631
445

Meier, H. E. M., Döscher, R., and Faxén, T. (2003). A multiprocessor coupled ice- ocean model for the Baltic Sea:
application to the salt inflow. Journal of geophysical research 108. doi:10.1029/2000JC000521

Meier, H. E. M. (2007). Modeling the pathways and ages of inflowing salt- and freshwater in the Baltic Sea. Estuarine,
450   Coastal and Shelf Science. https://doi.org/10.1016/j.ecss.2007.05.019

Meier, H. E. M., Eilola, K., Almroth-Rosell, E., Schimanke, S., Kniebusch, M., Höglund, A., et al. (2018). Disentangling the
impact of nutrient load and climate changes on Baltic Sea hypoxia and eutrophication since 1850. Climate Dynamics.
doi:https://doi.org/10.1007/s00382-018-4296-y
455

Munkes, B., Löptien, U., and Dietze, H. (2021). Cyanobacteria blooms in the Baltic Sea: a review of models and facts,
Biogeosciences, 18, 2347–2378, https://doi.org/10.5194/bg-18-2347-2021.

Nausch M, Nausch G, Mohrholz V, Siegel H, Wasmund N. (2012). Is growth of filamentous cyanobacteria supported by
460   phosphate uptake below the thermocline? Estuarine, Coastal and Shelf Science. 99: 50-60.

Nausch, M., Achterberg, E.P., Bach, L.T., Brussaard, C.P.D., Crawfurd, K.J., Fabian, J., Riebsell, U., Stuhr, A., et al. (2018). Concentrations and uptake of dissolved organic phosphorus compounds in the Baltic Sea. Frontiers in Marine Science 5: 386.

465

Olofsson, M., Egardt, J., Singh, A., and Ploug, H., (2016). Inorganic phosphorus enrichments in Baltic Sea water has large effects on growth, carbon fixation, and N2 fixation by *Nodularia spumigena*. Aquatic Microbial Ecology 77: 111–123.

Olofsson, M., Torstensson, A., Karlberg, M., Steinhoff, S.F., Dinasquet, J., Riemann, L., Chieric,i M., and Wulff, A. (2019).
470   Limited response of a spring bloom community inoculated with filamentous cyanobacteria to elevated temperature and *p*CO2. Bot Mar. 62(1): 3-16.

Olofsson, M., Suikkanen, S., Kobos, J., Wasmund, N., and Karlson, B. (2020). Basin-specific changes in filamentous cyanobacteria community composition across four decades in the Baltic Sea. Harm. Alg. 91: 101685.

475

Olofsson, M., Klawonn, I., and Karlson, B. (2021). Nitrogen fixation estimates for the Baltic Sea indicate high rates for the previously overlooked Bothnian Sea. AMBIO 50(1): 203-214.

Orlanski, I. (1976). A simple boundary condition for unbounded hyperbolic flows. Journal of Computational Physics
480   doi:10.1016/0021-9991(76)90023-1

Paerl, H.W., and Huisman, J., (2008). Blooms like it hot. Science 320: 57–58.

Ploug, H., Adam, B., Musat, N., Kalvelage, T., Lavik, G., Wolf-Gladrow, D., and Kuypers, M.M.M.(2011). Carbon,
485   nitrogen and O2 fluxes associated with the cyanobacterium *Nodularia spumigena* in the Baltic Sea. ISME Journal 5: 1549–1558.

Ploug, H., Musat, N., Adam, B., Moraru, C.L., Lavik, G., Vagner, T., Bergman, B., and Kuypers, M.M.M. (2010). Carbon and nitrogen fluxes associated with the cyanobacterium *Aphanizomeno*n sp. in the Baltic Sea. ISME Journal 4: 1215–1223.

490

Rakko, A. and Seppälä, J. (2014). Effect of salinity on the growth rate and nutrient stoichiometry of two Baltic Sea filamentous cyanobacterial species. Estonian Journal of Ecology doi:10.3176/eco.2014.2.01

Reusch, T.B.H., Dierking, J., Andersson, H.C., Bonsdorff, E. Carstensen, J., Casini M., Czajkowski, M, Hasler, B., et al.
495   2018. The Baltic Sea as a time machine for the future coastal ocean. Science Advances 4: eaar8195.

Rolff, C., Almesjö, L., and Elmgren, R. (2007). Nitrogen fixation and abundance of the diazotrophic cyanobacterium *Aphanizomenon* sp. in the Baltic Proper. Marine Ecology Progress Series 332: 107–118.

500   Saraiva, S., Meier, H. E. M., Andersson, H., Höglund, A., Dieterich, C., Gröger, M., et al. (2018). Baltic Sea ecosystem response to various nutrient load scenarios in present and future climates. Climate Dynamics 0, 1–19. doi:10.1007/s00382-018-4330-0

Schneider, B., Kaitala, S., Raateoja, M., and Sadkowiak, B. (2009). Nitrogen fixation estimate for the Baltic Sea based on
505   continuouspCO2 measurements on a cargo ship and total nitrogen data. Continental Shelf Research 29: 1535–1540.

Schoffelen, N. J., Mohr, W., Ferdelman, T. G., Littmann, S., Duerschlag, J., Zubkov, M. V., Ploug, H., & Kuypers, M. M. M. (2018). Single-cell imaging of phosphorus uptake shows that key harmful algae rely on different phosphorus sources for growth. Scientific Reports, 8(1), 1–13. https://doi.org/10.1038/s41598-018-35310-w

510

Sommer U, Aberle N, Langfellner K, Lewandowska A. (2012). The Baltic Sea spring phytoplankton bloom in a changing climate: an experimental approach. Mar Biol. 159: 2479-2490.

Steffen, W., Richardson, K., Rockström, J., Cornell, S.E., Fetzer, I., Bennett, E.M., Biggs, R., Carpenter, S.R., et al. 2015.
515   Planetary boundaries: Guiding human development on a changing planet. Science 347: 1259855.

Stevens, D. P. (1990). On open boundary conditions for three dimensional primitive equation ocean circulation models. Geophysical & Astrophysical Fluid Dynamics doi:10.1080/03091929008219853

520   Suikkanen, S., Kaartokallio, H., Hällfors, S., Huttunen, M., Laamanen, M., (2010). Life cycle strategies of bloom-forming, filamentous cyanobacteria in the Baltic Sea. Deep-Sea
Res. II 57, 199–209.

Svedén, J.B., Adam, B., Walve, J., Nahar, N., Musat, N., Lavik, G., Whitehouse, M.J., Kuypers, M.M.M., et al. (2015). High
525   cell-specific rates of nitrogen and carbon fixation by the cyanobacterium sp. at low temperatures in the Baltic Sea. FEMS Microbiology Ecology 91: fiv131.

Svedén, J.B., Walve, J., Larsson, U., and Elmgren, R. (2016). The bloom of nitrogen-fixing cyanobacteria in the northern Baltic Proper stimulates summer production. Journal of Marine Systems 163: 102–112.

530

Wannicke, N., Frey, C., Law, C.S., and Voss M. (2018). The response of the marine nitrogen cycle to ocean acidification. Global Change Biology 24: 5031–5043.

Wannicke, N., Koch, B.P., and Voss M. (2009). Release of fixed N2 and

535 C as dissolved compounds by *Trichodemsium erythreum* and *Nodularia spumigena* under the influence of high light and high nutrient (P). Aquatic Microbial Ecology 57: 175–189.

Wasmund, N., Voss, M., and Lochte, K. (2001). Evidence of nitrogen fixation by non-heterocystous cyanobacteria in the Baltic Sea and re-calculation of a budget of nitrogen fixation. Mar. Ecol. Prog. Ser. 214: 1–14.

540

Wasmund, N., Nausch, G., Schneider, B., Nagel, K., and Voss, M. (2005). Comparison of nitrogen fixation rates determined with different methods: A study in the Baltic proper. Mar. Ecol. Prog. Ser. 297: 23–31.

Wasmund, N. (2017). Recruitment of bloom-forming cyanobacteria from winter/ spring populations in the Baltic Sea

545 verified by a mesocosm approach. Boreal Environment Research 22, 445–455.

Wulff, A., Karlberg, M., Olofsson, M., Torstensson, A., Riemann, L., Steinhoff, S.F., Mohlin, M., Ekstrand, N., and Chierici, M. (2018). Ocean acidification and desalination: climate-driven change in a Baltic Sea summer microplanktonic community. Mar Biol 165: 63.
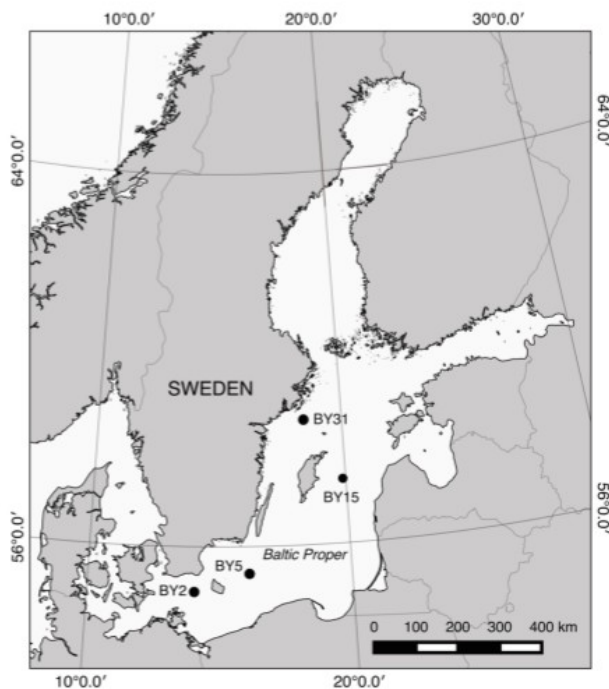
550   Figure 1. Map of the Baltic Sea. Baltic proper stations used in the study include BY31, BY15, BY5, and BY2.
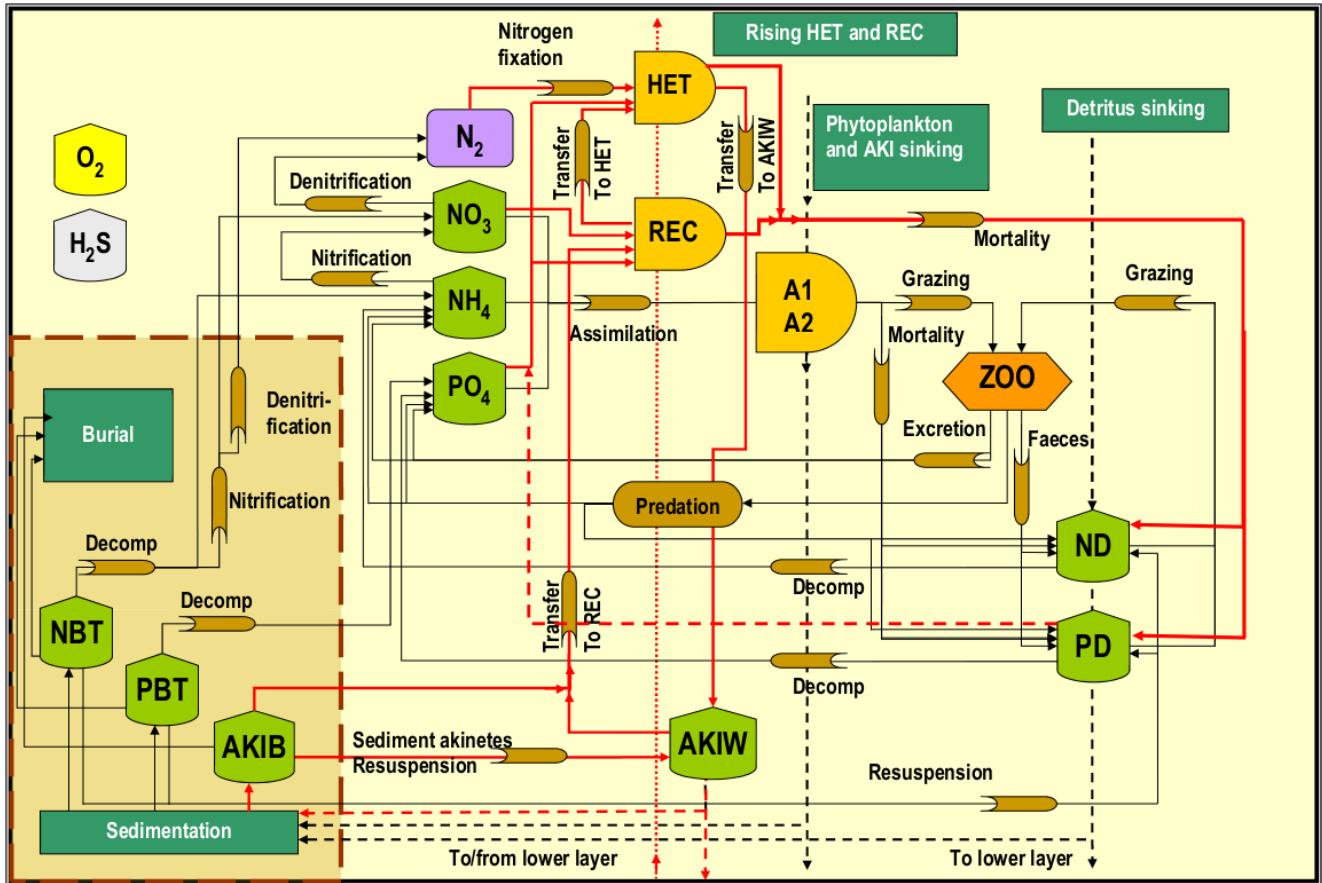
Figure 2. The SCOBI model including the cyanobacteria life cycle model components indicated by
555 red lines, vegetative cells with heterocysts (HET), Akinetes in water (AKIW) and in sediment
(AKIB), and Recruiting cells (REC). The inorganic nutrients nitrate, ammonia and phosphate are
represented by NO3, NH4 and PO4, respectively. The phytoplankton groups A1 and A2 represent
characteristics of diatoms and the flagellates and others. The bulk zooplankton ZOO grazes on
phytoplankton A1 and A2 while the parameterized predation closes the system of equations.
560 Nitrogen and phosphorus detritus are described by ND and PD, respectively. Oxygen dynamics are
included and hydrogen sulfide concentrations are represented by "negative oxygen equivalents (1
ml H2S l-1 = –2 ml O2 l-1). The process descriptions of oxygen and hydrogen sulfide are simplified
for clarity.
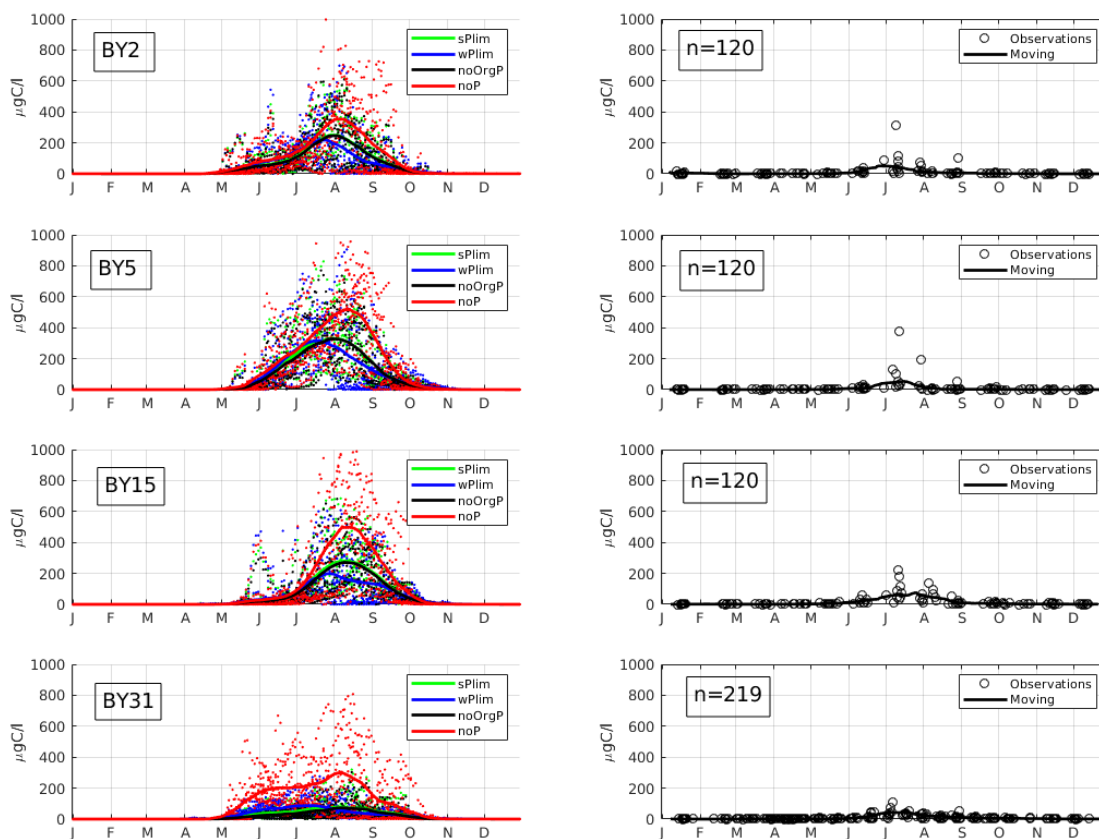
Figure 3. Mean seasonal cycle of cyanobacteria biomass for four different stations in the Baltic proper. Left panels show model results and the right panels observations. The number of observations is indicated by "n" in the right hand panels. Dots show model output for every two days and solid lines represent the one month moving average.
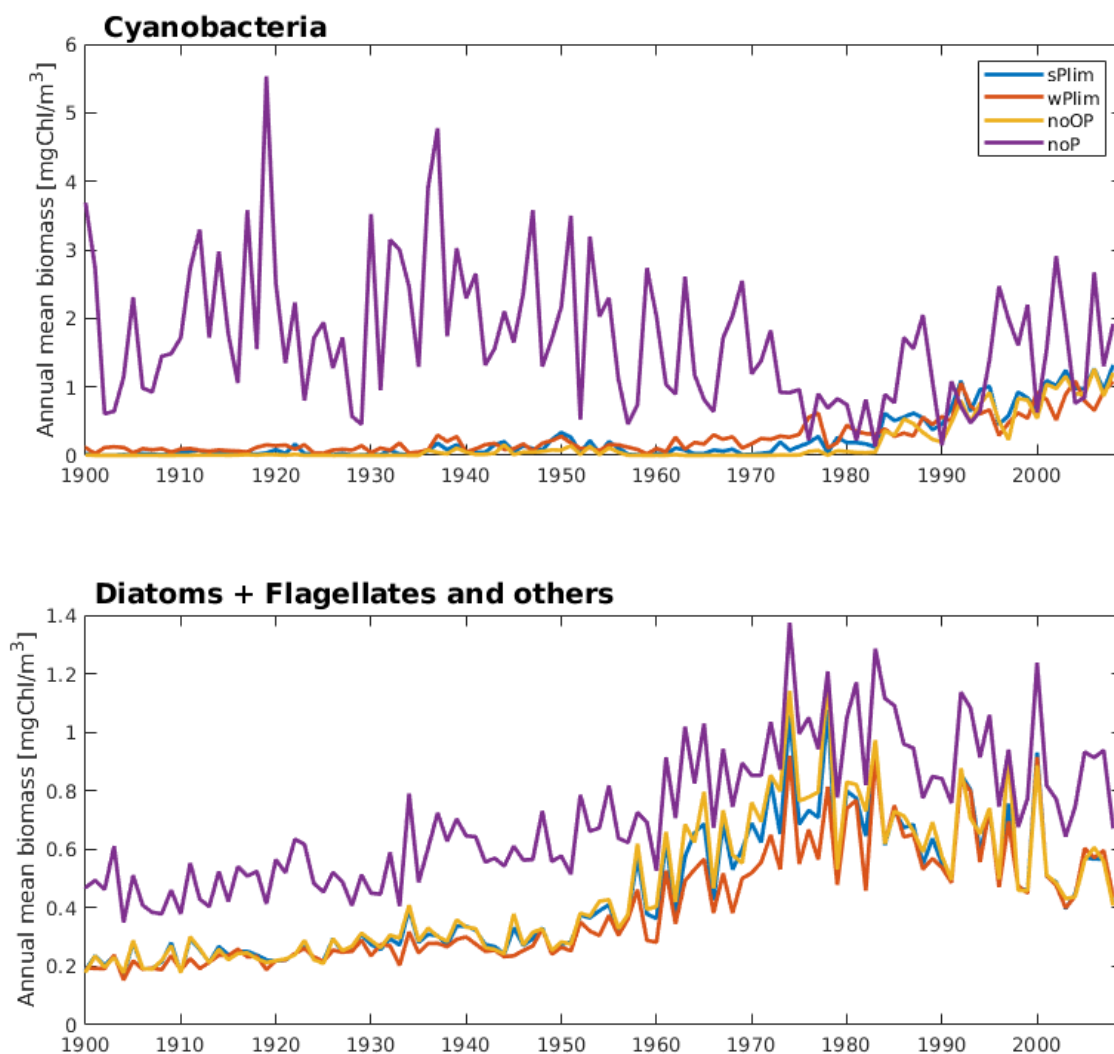
Figure 4. Simulated annual mean cyanobacteria biomass (upper) and the sum of annual mean biomass of functional types Diatoms and Flagellates and other autotrophic organisms (lower) at station BY15 for the four different sensitivity experiments.
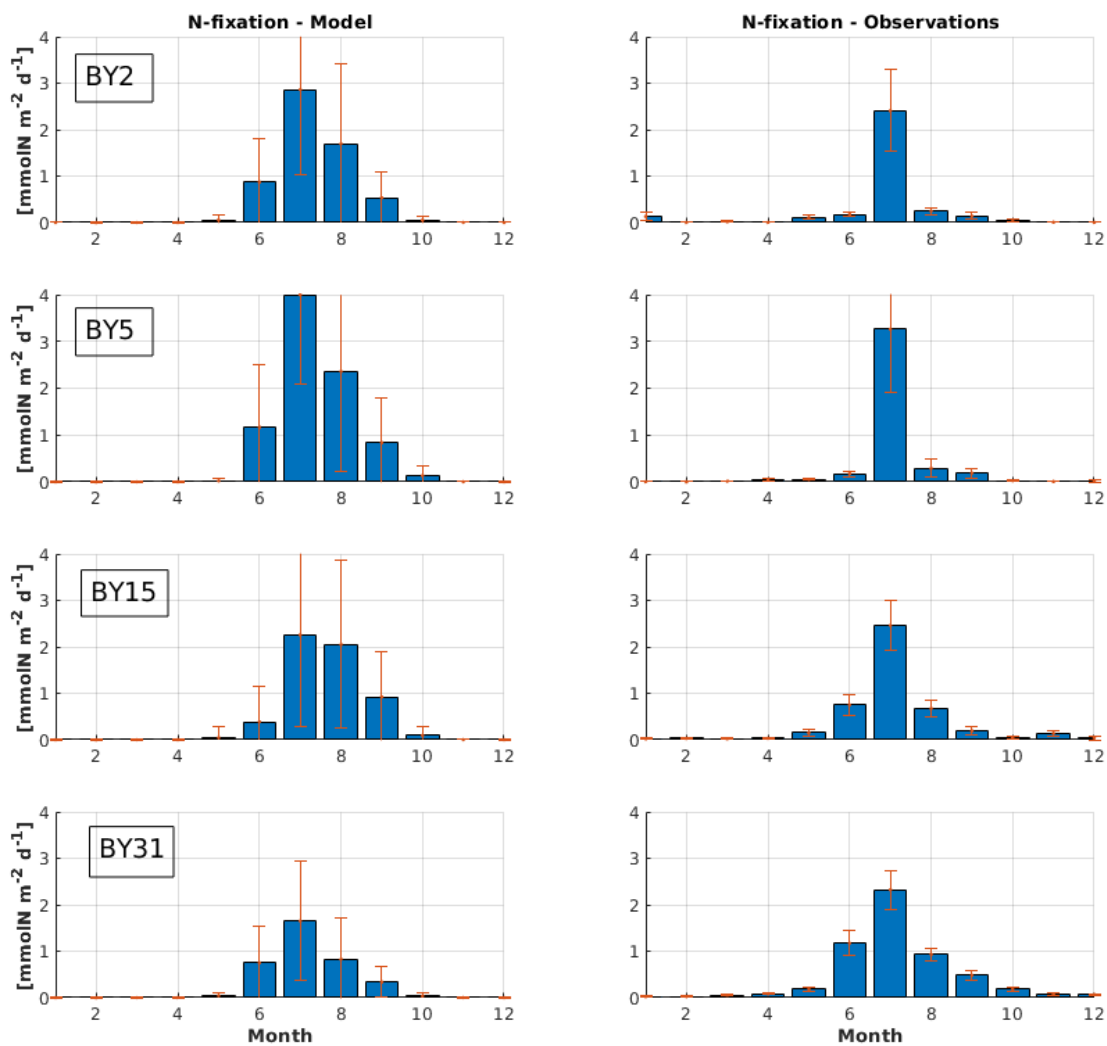
Figure 5. Model results (left) and observations (right) of mean seasonal nitrogen fixation rates over the years 1999-2008 at different stations using the wPlim phosphorus setting.

580
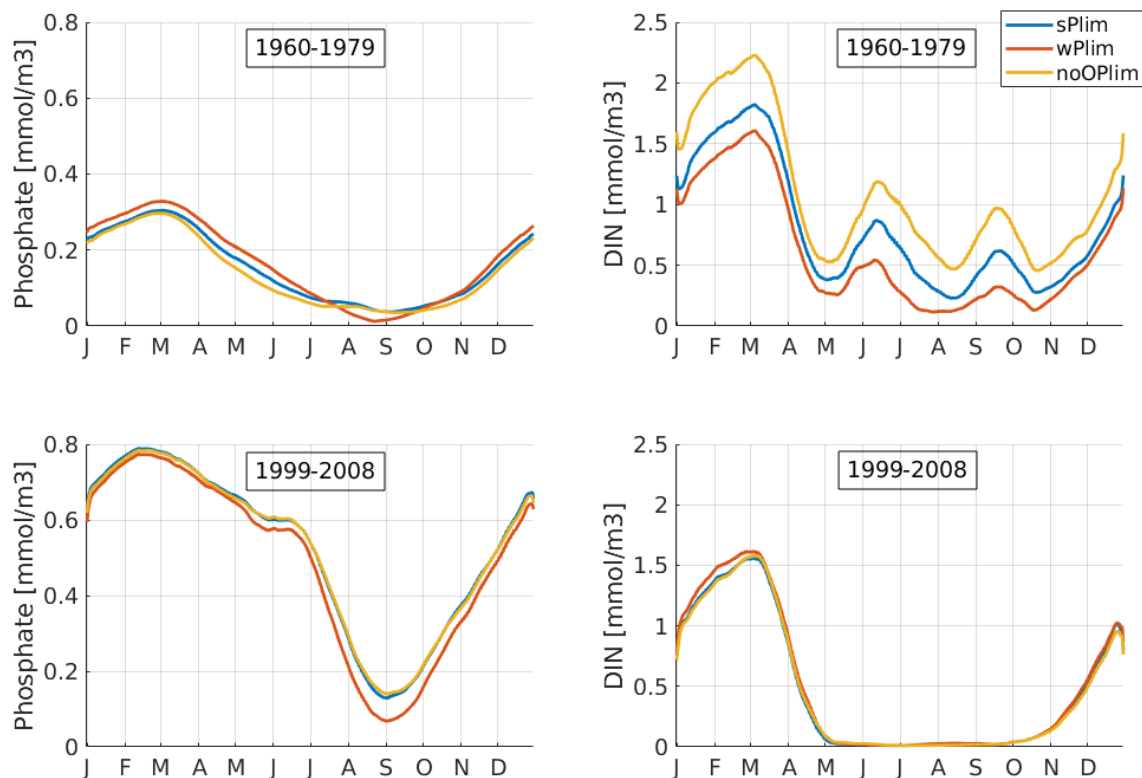
Figure 6. Mean seasonal cycle of surface phosphate (left) and DIN (right) at station BY15 for the period 1960-1979 (upper) and 1999-2008 (lower). The data-points have been smoothed using a 1 month moving average.

585

590
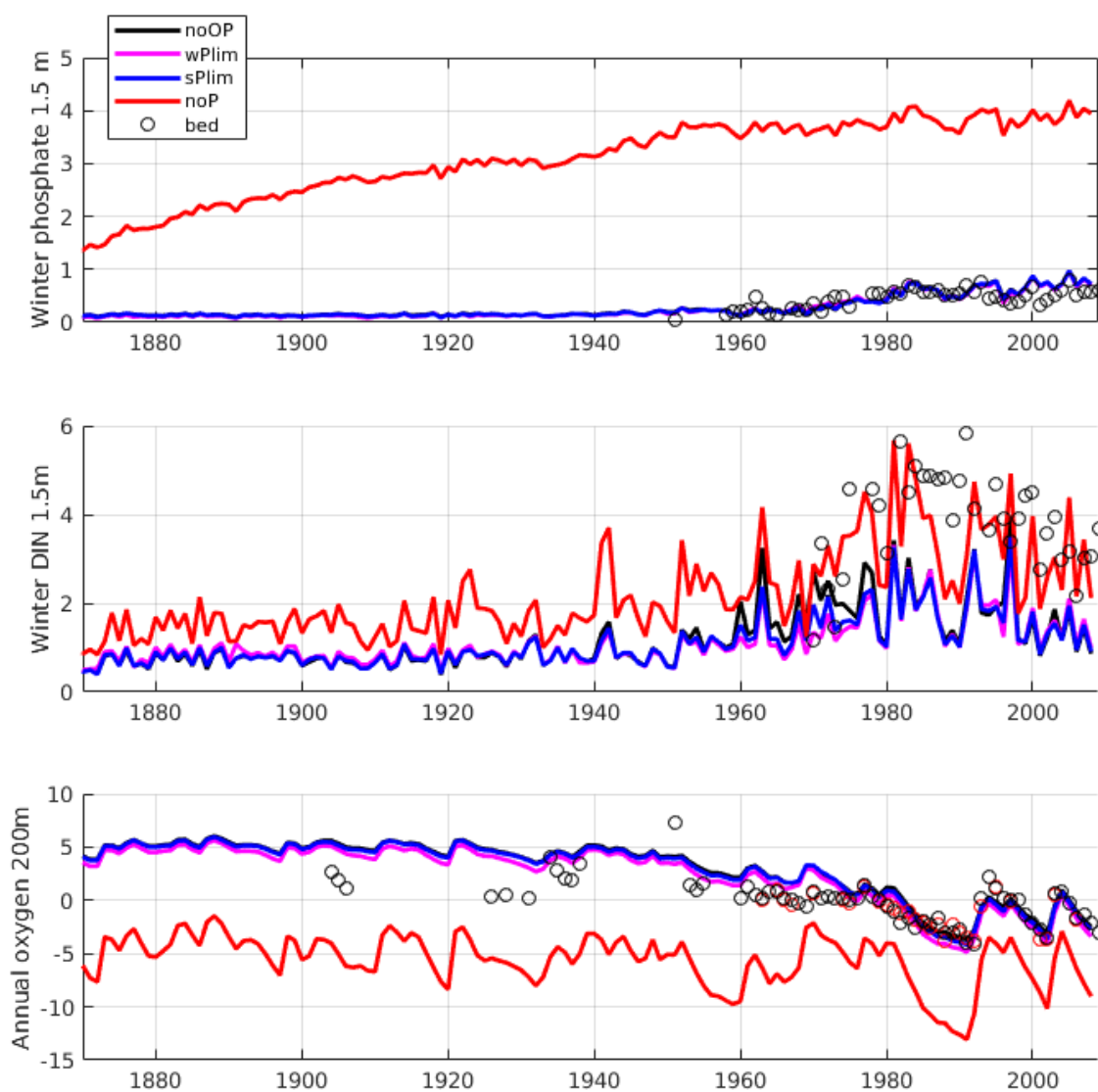
Figure 7. Evolution of winter (Jan-Feb) surface concentrations of phosphate (top), dissolved inorganic nitrogen (DIN; middle) and annual mean oxygen at 200m depth (bottom) at BY15. The solid lines show model results and the circles show observations from the Baltic Environmental Database (BED).
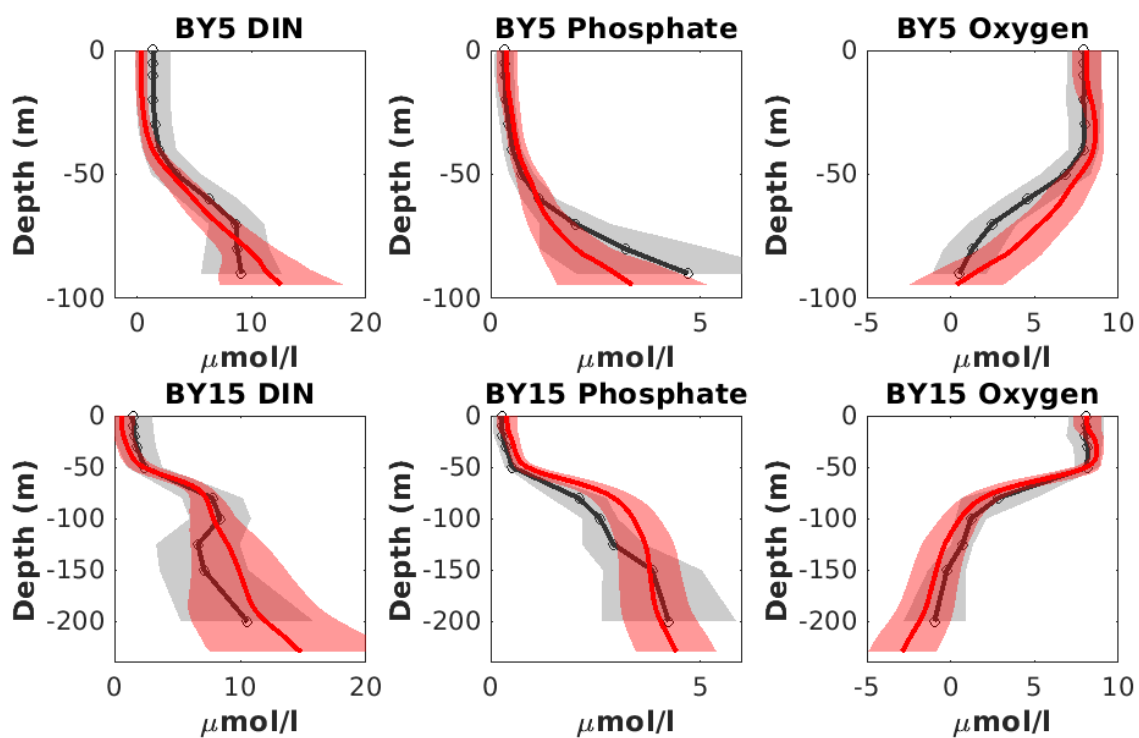
Figure 8. Profiles of DIN, phosphate and oxygen at BY5 (upper panels) and BY15 (lower panels) averaged over the years 1976 to 2008. Model data in red and observations from SHARK database in black. Shaded areas represent standard deviation.